Progress In Electromagnetics Research C, Vol. 55, 1–7, 2014

A Mini NMR Sensor for Monitoring the Degradation of Fire-Resistant Turbine Oils in Thermal Power Plant in Vivo

Pan Guo*, Wei He, and Zheng Xu

Abstract—Fire-resistant turbine oil is widely used in thermal power plant. As the service time increases, its lubrication and electrical characteristic degrade. This work proposes a mini NMR (nuclear magnetic resonance) sensor for assessing the degradation of the turbine oils used in real time and in vivo. Two magnetic discs with poles opposed were separated in a distance to generate a relative homogeneous static magnetic field between them. A solenoid coil was placed between the magnets as the RF coil. The dimensions of the sensor are 30 mm × 30 mm × 36 mm and the mass is 107 g. The T_1 and T_{2eff} of the turbine oils from two different power plants were measured. The results demonstrated that an increase of the service time of turbine oils clearly results in a decrease of T_1 and T_{2eff}. This method of monitoring degradation of turbine oils could lead to the use of NMR to assess the degradation level of turbine oils in service.

1. INTRODUCTION

In thermal power plant, the electrical energy delivered to the end customer is transformed from mechanical energy which is produced by thermal energy [1, 2]. The main equipment in charge of transforming thermal energy into mechanical energy is the turbine. With increment of power consumption, the control system of turbine has become increasingly complicated [3–6]. In the control system, turbine oils are used primarily for lubricating, cooling and vibration damping. The quality of turbine oils plays a crucial role in the control system. In order to enhance the fireproof ability, a phosphate ester fire-resistant oil has been widely used in most thermal power plants in the world [7–9].

When operating at high temperatures, in the presence of oxygen, water vapor and catalytically active metals, these fire-resistant turbine oils are severely stressed [10, 11]. These conditions will lead to a rapid degradation to the oils, which may cause corrosion and even failure of the system [12]. The aging status of the turbine oils may be roughly evaluated by observing the color and turbidity changes [1]. A more complicated routine detection requires operators to test the acidity, resistivity and impurities of the oil at least once a week [13–15]. Some sites even test the thermo-oxidative stability and corrosivity under simulated aging conditions, where the increase of acidity and viscosity, the formation of sludge and corrosion against various metals are controlled [16]. However, this method is expensive and time consuming and cannot be applied to a large number of samples in the surveillance of oils.

Since portable NMR sensor is simpler and much less expensive than traditional MRI (magnetic resonance imaging) system, it has been rapidly developed and become a powerful technique in different areas of application. Especially, portable NMR has performed very well recently to investigate materials aging and degradation [17, 18]. In previous work, we proposed a unilateral NMR sensor to investigate the degradation of fire-resistant turbine oils [19]. The result encouraged deep research to develop a mini NMR sensor for monitoring turbine oils in real time in vivo. The ultimate aim of this study is to

Received 11 September 2014, Accepted 2 November 2014, Scheduled 7 November 2014

* Corresponding author: Pan Guo (pan.guo.cq@gmail.com).

The authors are with the State Key Laboratory of Power Transmission Equipment & System Security and New Technology, Chongqing University, Chongqing 400044, China.

identify a potential method for regularly assessing the condition of a turbine oil so its aging degrees can be predicted and the replacement can be scheduled before catastrophic failure occurs.

The mini NMR sensor presented in this paper consists of two magnetic discs (with poles opposed) separated in a distance to generate a sensitive volume between them. A solenoid coil is employed as the RF coil for signal excitation and detection. In the following sections, the features of the sensor and the measurements on fire-resistant turbine oils are presented.

2. EXPERIMENTAL SECTION

2.1. Magnet

Different types of magnets can be employed for this kind of measurement. NMR spectrum analyzer works faster and gives more sensitive information of the samples, but it requires a more complicated design which costs much more than portable NMR. We designed a mini NMR sensor whose B_0 field is not so uniform in the sensitive volume. But considering its very small size ($30\,\text{mm} \times 30\,\text{mm} \times 36\,\text{mm}$) and mass (107 g), it is a good choice for the measurements in field and in vivo. In spite of simple structure, the mini NMR sensor produced reliable results.

Construction of the magnet body of the mini NMR sensor is depicted in Figure 1. It consists of two separated magnetic discs (with poles opposed) with two ferromagnetic washers below them to improve the homogeneity and enhance the magnetic field of the discs. Since the poles of the two magnets are opposed, in the measurement area, the magnetic field component perpendicular to the magnet surface generated by each magnet orients in the same direction, but the parallel components orient in the opposed direction. If the parallel components generated by each magnet can be cancelled, a relative homogeneous magnetic field would be generated. This idea can be worked out by adjusting the distance between the two magnets. N42 NdFeB magnetic discs and ferromagnetic washers (Lee Valley Tools Ltd., Ottawa, CA) were employed. The diameter and thickness were 25.4 mm, 3.2 mm for the magnets and 28.6 mm, 5.5 mm for the washers. The magnet design idea was verified through simulation (Vector Field Opera 12, Cobham Antenna Systems, Kidlington, Oxford, UK). The ideal distance (11 mm) between the magnets were therefore determined prior to prototype construction (Figure 1).

In order to characterize the magnet, magnetic field measurements were undertaken employing a 3D Gauss meter (Lake-Shore Cryotronics Inc., OH, USA). Figure 2 shows the magnetic field distribution along y axis and z axis corresponding to the coordinate system in Figure 1. In a $25\,\text{mm}^3$ sensitive volume at the centre of the magnet body, the calculated variation of the magnetic field was 0.74% (bandwidth is 80 kHz). The proton resonance frequency in this volume was thereby determined to be 10.5 MHz (where the B_0 was 0.25 T).

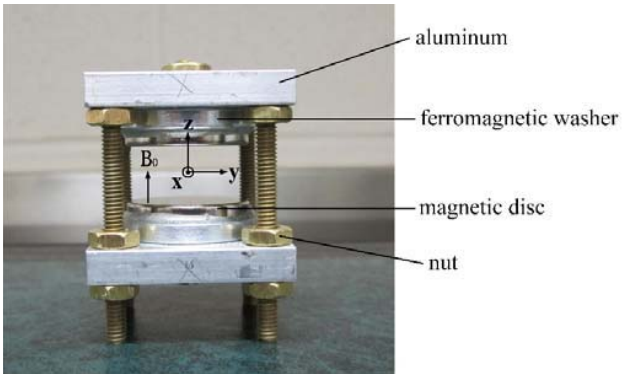

Figure 1. The magnet structure of the mini NMR sensor. The distance between the magnetic discs was adjusted by turning the nuts. The orientation of the B_0 field was perpendicular to the magnet surface.

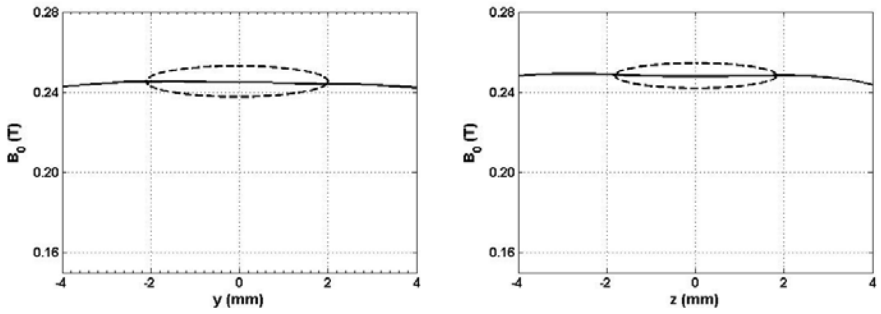

Figure 2. The solid line is the static magnetic field distribution of the sensor along (a) y and (b) z axis, and the area surrounded by the dash line is the sensitive volume.

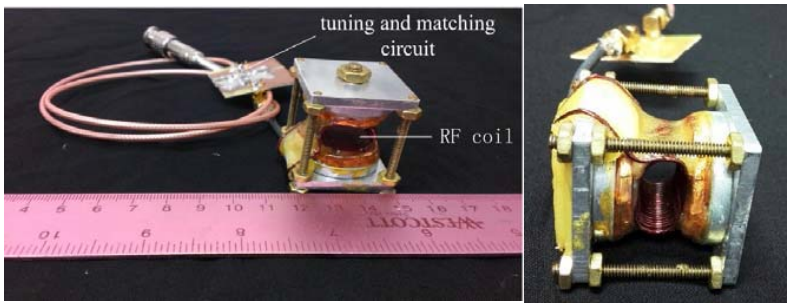

Figure 3. (a) A photo of the mini NMR sensor, RF coil and tuning circuit are marked. (b) A enlarged photo of the RF coil.

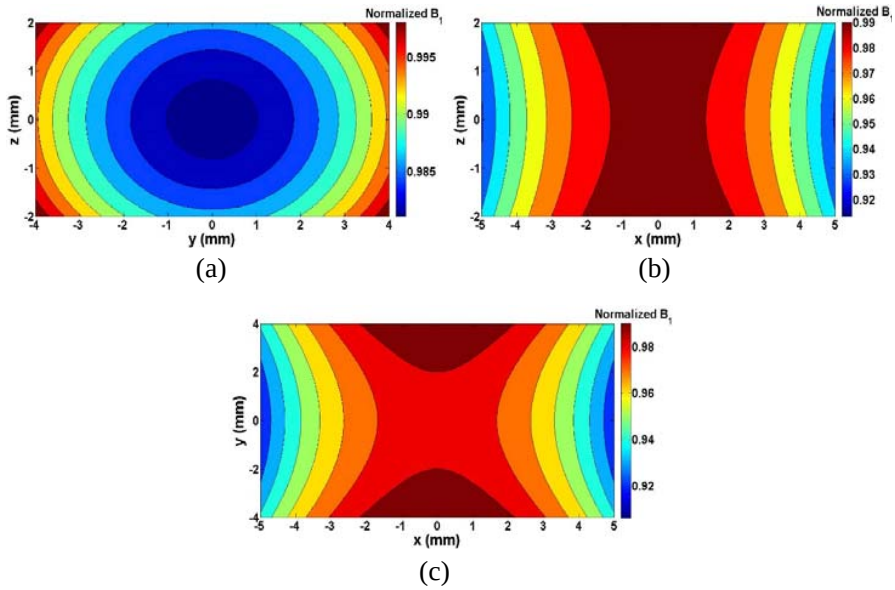

Figure 4. The simulated B_1 field distribution (a), (b), (c) of the RF coil. In the simulation, the current was set to be 1 A. The coordinate system was the same as in Figure 1.

2.2. RF Coil

A solenoid coil (Figure 3) was employed for the RF probe. Since the ideal gap (11 mm) between the magnets was less than the diameter of the magnets, in order to excite as much as possible samples to increase the signal strength, the RF coil was not a traditional solenoid coil. The cross section of the RF

coil was an ellipse with the semi-major axis 20 mm and semi-minor axis 10 mm. The RF coil was 18 mm in length with 11 turns (shown in Figure 3(b)). Between two turns of the RF coil, there was one turn of the wire without current for mechanical stability. The B_1 field inside the coil, simulated employing the simulation software Maxwell 3D (Ansoft, Pittsburgh, PA, USA), is shown in Figure 4.

The resistance and inductance of the coil were 1.1 Ω and 0.81 μH, respectively. The matching circuit was π type circuit, and the capacitance was 253 pF for tuning and 87 pF for matching. The loaded quality factor (Q_L), measured with the coil inserted between the magnets, was 68. The dead time of the RF probe was 33 μs. There was one layer of copper shield between the RF coil and the magnetic discs to avoid acoustic ringing.

2.3. Experimental Details

All measurements were carried out with a Kea2 console (Magritek, Wellington, New Zealand), connected to a RF power amplifier (TOMCO Technologies, Stepney, Australia) at 22 ± 0.3°C. The measurement system except the computer is shown in Figure 5.

In order to evaluate the effectiveness of the sensor, an eraser sample was employed for a CPMG (Carr-Purcell-Meiboom-Gill) measurement. The total measurement time was less than 10 s.

Two groups of fire-resistant turbine oils (Table 1), collected from two different power stations, were detected. The oils are shown in Figure 6. The sensor was immersed into the oil samples. The ^{1}H NMR effective transverse relaxation time (T_{2eff}) and longitudinal relaxation time (T_1) were obtained with the standard CPMG sequence and T_1 Inversion Recovery with CPMG (T_1 IR Add) sequence, respectively. The main parameters of all the sequences are shown in Table 2. The power employed for the 90° pulse was 6.3 Watt which was a half of the power for the 180° pulse. The total measurement time was 1 min for T_{2eff}, 5 min for T_1.

All experimental decay measurements were fit to mono-exponential decay and bi-exponential decay with nonlinear regression in Sigmaplot 12.0 (Systat Software Inc., San Jose, CA, US), as well as multi-exponential decay with Contin program.

Figure 5. A photo of the measurement system, the sensor was immersed into the turbine oil.

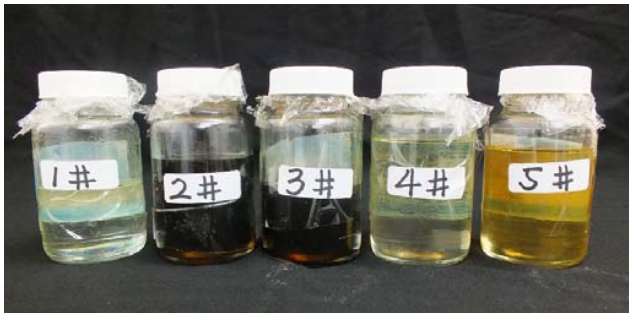

Figure 6. Turbine oil samples with the numbers labeled.

Table 1. Turbine oils for the measurements.

Power Plant Name	Number	Status
Beilun	1 #	New
	2 #	In service
	3 #	Aged
Yuyao	4 #	New
	5 #	In service

Table 2. Main parameters of the sequences for all the measurements.

Sample	Sequence	PW (μs)	90° (dB)	180° (dB)	TE (μs)	NE	t_r (ms)	NS
Eraser	CPMG	13	−19	−13	130	700	200	32
Oil	CPMG	13	−19	−13	130	3000	550	64
Oil	T_1 IR Add	13	−19	−13	130	64	550	16

Note: PW is the pulse width; 90° and 180° are the attenuations of the pulses; TE is echo time; NE is the number of echoes; t_r is the repetition time; NS is the number of scans.

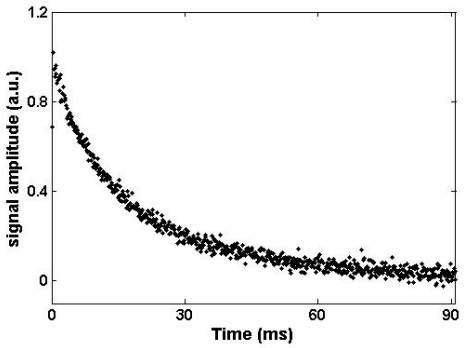

Figure 7. A CPMG decay obtained from the eraser sample. 32 scans were averaged.

3. RESULTS AND DISCUSSION

3.1. Sensitivity Test

Figure 7 shows the CPMG decay obtained with the mini NMR sensor from the eraser sample. 32 scans were averaged. The signal to noise ratio, which is the signal intensity divided by the noise level, was 24. Three repeated measurements with the sensor on the eraser sample yielded less than 0.5% standard deviation.

Since the static magnetic field is less homogeneous in the mini NMR than in commercial NMR, this paper does not consider the influence of the magnetically susceptibility of the sample on the sensitivity of the sensor.

3.2. Effective Transverse Relaxation Time Measurements

In inhomogeneous static magnetic fields, it is not possible to obtain a pure T_2 decay from a CPMG echo train. Because of the static magnetic field inhomogeneities, the RF pulses excite multiple coherence pathways simultaneously; therefore the decay time constant is a weighted sum of the $1/T_1$ and $1/T_2$ relaxation rates which is called effective transverse relaxation time T_{2eff} [20].

The CPMG echo trains were fitted by mono-exponential model (Eq. (1)), bi-exponential model (Eq. (2)) and multi-exponential model (inverse Laplace transform with Contin program) to extract the effective lifetimes T_{2eff}.

$$M(t) = A \cdot \exp\left(-\frac{t}{T_{2eff}}\right) + Noise \tag{1}$$

$$M(t) = A_{short} \cdot \exp\left(-\frac{t}{T_{2eff,short}}\right) + A_{long} \cdot \exp\left(-\frac{t}{T_{2eff,long}}\right) + Noise \tag{2}$$

Comparing the standard errors of the three fitting results, it was found that mono-exponential fitting was more precise. Table 3 shows the mean T_{2eff} with the associated variations of the three repeated measurements for each sample.

It can be inferred from the result that the aging status of different turbine oils can be distinguished in the measured T_{2eff} and an increase in service time yields a decrease in effective transverse relaxation

Table 3. The mean T_{2eff} of each sample and the variations.

Number	T_{2eff} (ms)	Variation (ms)
1 #	87.2	±0.06
2 #	85.0	±0.03
3 #	83.0	±0.06
4 #	84.2	±0.07
5 #	81.6	±0.04

Table 4. The mean T_1 of each sample and the variations.

Number	T_1 (ms)	Variation (ms)
1 #	99.2	±0.14
2 #	96.3	±0.31
3 #	90.3	±0.13
4 #	97.3	±0.17
5 #	86.2	±0.13

time T_{2eff}. This result agrees with the effective transverse relaxation time measurements of the previous work. Nevertheless, the variations of T_{2eff} of this method are one order less than unilateral magnetic resonance method in previous work, which means a less noise level of the mini NMR sensor.

3.3. Longitudinal Relaxation Time Measurements

For measuring T_1 in inhomogeneous magnetic field, a standard inversion recovery with CPMG detection added (T_1-IR-Add) sequence was employed. This can results in a considerable improvement in signal to noise ratio when compared with the simpler T1-IR-Echo experiment. Since the mono-exponential decay fitting was more precise for T_{2eff}, the integrals of the CPMG echoes were also fitted to Eq. (1). Table 3 shows the mean T_1 with the associated variations of the three repeated measurements for each sample.

From Table 4, an increase in the service time yields a decrease in longitudinal relaxation time T_1 of turbine oils. This result agrees with the T_1 measurements of the previous work. Nevertheless, the variations of T_1 of this method are one order less than unilateral magnetic resonance method in previous work. It must be noticed that the reproducibility of T_{2eff} measurements are better than T_1 measurements.

To obtain a quantitative relation between the NMR testing and the disable degree of the turbine oils, we will employ the new turbine oil as the reference sample. Firstly, we will measure T_{2eff} and T_1 of the new turbine oil. Secondly, we will measure T_{2eff} and T_1 of the aged turbine oil. Finally, the differences of T_{2eff} and T_1 between the new and aged turbine oils will be divided into 5 (whatever) degrees. Therefore, we get the T_{2eff} and T_1 ranges of different aging degrees of the turbine oil. Once we measure the T_{2eff} and T_1 of any turbine oil, we can know the aging degree of it. It should be noted that all the turbine oils samples tested above should be the same type. This work needs to measure a number of turbine oils to get the range of T_{2eff} and T_1 for different aging degrees which will be done in the future.

4. CONCLUSION

In previous work, it has been shown that unilateral magnetic resonance is a technique that can be used to quantify the level of degradation of fire-resistant turbine oils. In this work, a mini NMR sensor was employed for measuring the turbine oils by immersed the sensor into the samples. The measurement results also showed to be sensitive to changes due to aging in turbine oils. We demonstrate that the aging results in a decrease in T_1 and T_{2eff}. Moreover, the mini NMR sensor performed much better on the signal to noise ratio and the stability of the measurements. This technique could lead to monitoring aging of turbine oils in power stations in real time and predicting when these turbine oils should be replaced to prevent unexpected failure.

ACKNOWLEDGMENT

This work was financially supported by the Chinese 973 program (2014CB541600), the National Natural Science Foundation of China (51107150 and 51377186), and the Scientific Research Foundation of State Key Lab of Power Transmission Equipment and System Security (2007DA10512713103). Pan Guo thanks Dr. Juan C. García-Naranjo and Mr. Rod MacGregor for assisting on building the sensor.

REFERENCES

1. Liu, Y. L., "The application of phosphate ester hydraulic fluid in Chinese power industry," *Lubricating Oil*, Vol. 21, No. 5, 9–13, 2006.
2. Shi, Q. G., "Frameworks of energy audit for thermal power plants," *Journal of Shanghai University of Electric Power*, Vol. 25, No. 5, 500–504, 2009.
3. Griffin, T., S. G. Sundvist, K. Asen, and T. Bruun, "Advanced zero emissions gas turbine power plant," *Journal of Engineering for Gas Turbines and Power*, Vol. 127, No. 1, 81–85, 2005.
4. Wächter, C., R. Lunderstädt, and F. Joos, "Dynamic model of a pressurized SOFC/Gas turbine hybrid power plant for the development of control concepts," *Journal of Fuel Cell Science and Technology*, Vol. 3, No. 3, 271–279, 2006.
5. Masoumi, E., G. H. Farrahi, K. A. Masoumi, A. A. Zare, and S. Parsa, "Failure analysis of a gas turbine compressor in a thermal power plant," *Journal of Failure Analysis and Prevention*, Vol. 13, No. 3, 313–319, 2013.
6. Jericha, H., V. Hacker, W. Sanz, and G. Zotter, "Thermal steam power plant fired by hydrogen and oxygen in stoichiometric ratio, using fuel cells and gas turbine cycle components," *Proceedings of the ASME Turbo Expo*, Vol. 3, 513–520, 2010.
7. Cooper, T. and K. Ullmann, "Fire loss history and advances in fire protection for US based electric utilities," *VGB PowerTech*, Vol. 80, No. 8, 19–21, 2000.
8. Vilyanskaya, G. D., V. V. Lysko, and M. S. Fragin, "Improving fire prevention in turbine plants by using fire-resistant oils," *Thermal Engineering*, Vol. 35, No. 4, 193–195, 1988.
9. Vilyanskaya, G. D., V. V. Lysko, M. S. Fragin, and A. G. Vainstein, "VTI fire-resistant turbine oils and the part played by them in increasing fire protection at thermal and nuclear power stations," *Thermal Engineering*, Vol. 38, No. 7, 38–41, 1991.
10. Zhang, X. M., J. Yuan, B. Chen, P. Li, Y. B. Zhang, and L. C. Wang, "Cause of quality degradation and dehydration purification technology of phosphate ester fire-resistant oil," *Environmental Science Technology*, Vol. 35, 129–133, 2012.
11. Huang, W. Q., "Degradation reason of EH fire-resistant oil and regeneration," *Power Equipment*, Vol. 3, 216–218, 2010.
12. Yan, B., X. D. Lai, J. H. Long, X. Huang, and F. Hao, "Dynamic characteristics analysis of an oil turbine," *2012 International Conference on Modern Hydraulic Engineering*, Vol. 28, 12–17, 2012.
13. McDonald, C. F. and J. A. Paget, "Maintenance considerations in the design of the direct-cycle nuclear gas turbine power plant," *American Society of Mechanical Engineers*, 79-GT-116, 1979.
14. Günther, R., "Operating Experience with Synthetic Fluids in the Control and Governing Systems of Steam Turbines," *VGB PowerTech*, Vol. 77, No. 12, 930–934, 1997.
15. Dong, Z. Q., "The operation and maintenance for the oil used in regulating system of steam turbine," *Northeast Electric Power Technology*, Vol. 3, 12–14, 2001.
16. Bartl, P., K. Zuber, M. Leipold, and A. Zeman, "Quality control of used synthetic aviation turbine oils by analytical methods. I. Determination of the antioxidative capacity by HPLC and GC," *Fresenius' Zeitschrift für Analytische Chemie*, Vol. 314, No. 1, 25–28, 1983.
17. Xu, Z., S. J. Zhao, and P. Guo, "A portable NMR sensor used for assessing the aging status of silicone rubber insulator," *Applied Magnetic Resonance*, Vol. 44, 1405–1417, 2013.
18. Somers, A. E., T. J. Bastow, M. I. Burgar, M. Forsyth, and A. J. Hill, "Quantifying rubber degradation using NMR," *Polymer Degradation and Stability*, Vol. 70, 31–37, 2000.
19. Guo, P., W. He, and J. C. García-Naranjo, "Degradation of phosphate ester hydraulic fluid in power station turbines investigated by a three-magnet unilateral magnet array," *Sensors*, Vol. 14, 6797–6805, 2014.
20. Hurlimann, M. D., "Well logging," *Encyclopedia of Magnetic Resonance*, 1–10, Wiley, New York, 1996.